

Stratified stochastic variational inference for high-dimensional network factor model

Emanuele Aliverti¹ and Massimiliano Russo²

¹*Department of Statistical Sciences, University of Padova, Padova, Italy*

²*Harvard-MIT Center for Regulatory Science, Harvard Medical School & Department of Data Sciences
Dana-Farber Cancer Institute, Boston, USA*

Abstract

There has been considerable recent interest in Bayesian modeling of high-dimensional networks via latent space approaches. When the number of nodes increases, estimation based on Markov Chain Monte Carlo can be extremely slow and show poor mixing, thereby motivating research on alternative algorithms that scale well in high-dimensional settings. In this article, we focus on the latent factor model for networks, a very general approach which encompasses the latent distance model and the stochastic block-model as special cases. We develop scalable algorithms to conduct approximate Bayesian inference via stochastic optimization. Leveraging sparse representations of network data, the proposed algorithms show massive computational and storage benefits, and allow to conduct inference in settings with thousands of nodes. We provide an R package with an efficient C++ implementation of the proposed algorithms at github.com/emanuelealiverti/svilf, along with a tutorial to replicate the results of the article.

Keywords: High-dimensional networks; Latent Factor Model; Sparsity; Stochastic optimization; Variational Inference.

1 INTRODUCTION

Network data are routinely collected and analyzed in different fields of science; for example, neuroscience (Bullmore and Sporns, 2009), genetics (Wu et al., 2008) and epidemiology (Keeling and Eames, 2005), among many others. Refer also to Newman (2018) for an introduction to network data and their analysis. One of the main goals in network data analysis is to characterize the geometry underlying node relationships, providing a parsimonious, yet flexible, representation of the connectivity patterns. This goal can be achieved modeling the connectivity architectures in terms of a low-dimensional latent structure, where

the edges are represented as conditionally independent random variables given a set of latent coordinates (e.g., Hoff et al., 2002; Airoldi et al., 2008). Beside improving computation, these approaches provide concrete benefits in interpretation; for example, the latent structure can be related with observable covariates to improve the understanding of connectivity patterns, or divided into clusters to detect nodes that behaves similarly in terms of their unobservable features (e.g., Aliverti and Durante, 2019). The increasing availability of network data has further motivated the development of novel latent structures models for networks, covering more complex settings such as dynamic networks (e.g., Sewell and Chen, 2015), multi-layer networks (e.g., D’Ángelo et al., 2019) and populations of networks (Durante et al., 2017). Since the number of edges grows quadratically with the number of nodes, representing the latent structure of a network is computationally challenging, even for networks with few hundred nodes. This issue stimulates the development of novel methods and computational routines to accommodate large network structures efficiently, leveraging different network properties—such as sparsity or block structures—to facilitate computations. For example, large network data are often very sparse, with the number of observed edges being much smaller than the total number of possible connections. This feature allows to parsimoniously store network data via sparse matrix representations, or, equivalently, edge-lists formats (e.g. Csardi and Nepusz, 2006). However, estimation of latent structure models often requires edge-specific operations, lowering the benefits of these representations; see for example Airoldi et al. (2008) and Ho et al. (2016) for related arguments. In addition, most inference procedures for latent space models are based on Markov Chain Monte Carlo (MCMC) algorithms (e.g., Hoff, 2019), and these methods scale poorly with the number of nodes. Therefore, Bayesian inference for latent space models is often limited to networks with hundreds of nodes (Hoff, 2019).

There have been some attempts to improve computational efficiency and mixing of MCMC for latent space model for networks. For example, Raftery et al. (2012) derive an unbiased estimator of the log-likelihood based on an informative subset of nodes, and successfully perform MCMC estimation in an application with roughly three thousands nodes (Raftery et al., 2012, section 4.2). Although this approach effectively reduces the cost of each likelihood evaluation, inference is still computationally demanding; the algorithm requires a preliminary pilot MCMC run and a considerable amount of storage to perform Monte Carlo integration.

These computational issues motivate the development of scalable methods for approximate Bayesian inference, with Variational Bayes (VB) being a popular option. Specifically, VB algorithms approximate the posterior distribution via optimization, estimating the closest member (in Kullback-Liebler divergence)

within a pre-specified class of distributions. This class includes some restrictions to achieve computational tractability; for example, the resulting approximate posterior distribution factorizes in independent blocks of parameters (mean-field VB), or follows a specific parametric form (e.g., multivariate Gaussian). Refer to Blei et al. (2017) and references therein for more details. To date, the currently available VB routines for latent space models (Gollini and Murphy, 2016; Salter-Townshend and Murphy, 2013) are based on restrictive assumptions on the functional form of the variational distributions and rely on approximations of the complete log-likelihood function (Gollini and Murphy, 2016). In addition, these algorithms encounter computational issues in high-dimensional settings, since they scale quadratically with the number of nodes (Salter-Townshend and Murphy, 2013).

In this paper, we focus on the Latent Factor Model for binary undirected networks, a very general approach which includes the stochastic-block model and the latent distance model as special cases (Hoff, 2008). We propose scalable algorithms based on a stratified stochastic variational approximation for the LFM, which we refer to as SVILF in the sequel. From a computational perspective, SVILF explicitly relies on sparse network representations via edge-lists, which allows to scale up computations for networks consisting of thousands of nodes with low memory requirements. Leveraging a conditionally conjugate exponential family representation, we provide a unified framework for the LFM with logistic and probit link function and illustrate how SVILF can be directly implemented under both specifications.

2 METHODS

2.1 Latent Factor Model

Let \mathbf{Y} denote an $n \times n$ binary symmetric adjacency matrix with elements $y_{ij} = y_{ji} = 1$ denoting the presence of an edge between node i and node j with $i = 2, \dots, n$ and $j = 1, \dots, i - 1$, and $y_{ij} = y_{ji} = 0$ otherwise. The Latent Factor Model for networks (LFM, Hoff, 2005, 2008) parametrizes the edges as conditional independent Bernoulli random variables given a set of latent positions $\mathbf{w}_i = (w_{i1}, \dots, w_{iH}) \in \mathbb{R}^H$, $i = 1, \dots, n$. This choice implies

$$(y_{ij} \mid \pi_{ij}) \sim \text{Ber}(\pi_{ij}), \quad g(\pi_{ij}) = \mathbf{w}_i^\top \mathbf{w}_j = \sum_{h=1}^H w_{ih} w_{jh}, \quad i = 2, \dots, n, j = 1, \dots, i - 1, \quad (1)$$

where $g : [0, 1] \rightarrow \mathbb{R}$ is a monotone link function. Popular choices for g include the logit and probit link, which correspond to the inverse of the cumulative distribution function of a standard logistic and a standard Gaussian random variables, respectively (e.g., Agresti, 2015). See also Young and Scheinerman

(2007) for alternative specifications of the model outlined in Equation (1). In a Bayesian setting, we typically assign independent Gaussian priors to the latent factors, thereby letting $\mathbf{w}_i \sim N_H(\mathbf{a}_0, \mathbf{I}_H)$ for $i = 1, \dots, n$. A prior mean $\mathbf{a}_0 = (a_{01}, \dots, a_{0H})$ different from zero allows to center the factors around an expected network sparsity, accounting for the baseline probability of observing a connection. According to Equation (1), the probability of observing a connection between node i and node j depends on their latent positions \mathbf{w}_i and \mathbf{w}_j . The more similar node i and node j are in the latent space, the more likely it is to observe an edge connecting them. The similarity between two nodes in the latent space is computed with the multiplicative effect $\mathbf{w}_i^\top \mathbf{w}_j$, and this measure is particularly helpful in characterizing transitivity and uncovering group structures (Hoff, 2019). The LFM reduces the number of free parameters needed to characterize the network from $n(n-1)/2$ to nH , providing a low-dimensional representation of the connectivity patterns. Additionally, the LFM is a very general class of latent structure models for networks, and includes the latent distance model (Hoff et al., 2002) and the stochastic block models (Nowicki and Snijders, 2001) as special cases (Hoff, 2008). For these reasons, the LFM has been used as a building block for several generalizations involving multiple, time-varying, and covariate-dependent networks, among others (e.g., Durante et al., 2017; Sewell and Chen, 2015). Therefore, efficient algorithms for the LFM are crucial to analyze large network data, which are routinely collected in different fields of application.

Recalling Equation (1), it is worth highlighting that the predictor $g(\pi_{ij})$ is linear in the latent factors. Focusing on a single factor \mathbf{w}_i , we can recast the model outlined in Equation (1) as a conditional binary regression, given the other factors \mathbf{w}_j , $j \neq i$. Denoting with $\mathbf{y}_i = (y_{i1}, \dots, y_{ii-1}, y_{ii+1}, \dots, y_{in})$ the i -th row of the adjacency matrix \mathbf{Y} , with $\boldsymbol{\pi}_i = (\pi_{i1}, \dots, \pi_{ii-1}, \pi_{ii+1}, \dots, \pi_{in})$ the $(n-1)$ -variate vector of associated edge probabilities and with \mathbf{W}_{-i} the $(n-1) \times H$ dimensional matrix obtained stacking the factors $\{\mathbf{w}_j\}_{j \neq i}$, it holds that

$$g(\boldsymbol{\pi}_i) = \mathbf{W}_{-i} \mathbf{w}_i, \quad (2)$$

where the link function $g(\cdot)$ in Equation (2) is applied element-wise.

Equation (2) allows one to rely on iterative algorithms for posterior inference under the LMF, considering n binary regressions where each factor acts, in turn, as a regression coefficients. Moreover, for some specific link functions g , data-augmentation schemes are available to further simplify posterior inference. For the specific case of the LFM under the logit or probit link function g , introducing a set of latent variables z_{ij} , $i = 2, \dots, n$ and $j = 1, \dots, i-1$, conditional conjugacy between the Gaussian priors for \mathbf{w}_i and the

Bernoulli likelihood can be obtained, facilitating the updates of each \mathbf{w}_i .

Specifically, with the logit link function conditional conjugacy can be retrieved relying on the Pòlya-Gamma (PG) data augmentation strategy introduced by Polson et al. (2013), that leads to the following full conditionals distributions:

$$\begin{aligned} (z_{ij} \mid \mathbf{w}_i, \mathbf{w}_j, y_{ij}) &\sim \text{PG}(1, \mathbf{w}_i^\top \mathbf{w}_j), \quad i = 2, \dots, n, \quad j = 1, \dots, i-1, \\ (\mathbf{w}_i \mid \mathbf{W}_{-i}, \mathbf{z}_i, \mathbf{y}_i) &\sim \text{N}(\boldsymbol{\mu}_{\mathbf{w}_i}, \boldsymbol{\Sigma}_{\mathbf{w}_i}), \quad i = 1, \dots, n, \end{aligned} \quad (3)$$

where

$$\boldsymbol{\Sigma}_{\mathbf{w}_i} = (\mathbf{W}_{-i}^\top \text{diag}(\mathbf{z}_i) \mathbf{W}_{-i} + \mathbf{I}_H)^{-1}, \quad \boldsymbol{\mu}_{\mathbf{w}_i} = \boldsymbol{\Sigma}_{\mathbf{w}_i} (\mathbf{W}_{-i}^\top (\mathbf{y}_i - 0.5 \cdot \mathbf{1}_{n-1}) + \mathbf{I}_H \mathbf{a}_0),$$

and with $\mathbf{z}_i = (z_{i1}, \dots, z_{ii-1}, z_{ii+1}, \dots, z_{in})$. In Equation (3), $\text{PG}(c, d)$ denotes the density of a Pòlya-Gamma distribution with parameters c and d ; refer to Polson et al. (2013) for more details.

Similarly, with the probit link function, conditional conjugacy is obtained adapting the data-augmentation proposed in Albert and Chib (1993), which introduces auxiliary observations distributed as truncated normal random variables. The full conditional distributions under this specification correspond to

$$\begin{aligned} (z_{ij} \mid \mathbf{w}_i, \mathbf{w}_j, y_{ij}) &\sim \begin{cases} \text{TN}(\mathbf{w}_i^\top \mathbf{w}_j, 1, [0, +\infty]), & \text{if } y_{ij} = 1 \\ \text{TN}(\mathbf{w}_i^\top \mathbf{w}_j, 1, [-\infty, 0]), & \text{if } y_{ij} = 0 \end{cases} \quad i = 2, \dots, n, \quad j = 1, \dots, i-1, \\ (\mathbf{w}_i \mid \mathbf{W}_{-i}, \mathbf{z}_i, \mathbf{y}_i) &\sim \text{N}_H(\boldsymbol{\mu}_{\mathbf{w}_i}, \boldsymbol{\Sigma}_{\mathbf{w}_i}), \quad i = 1, \dots, n, \end{aligned} \quad (4)$$

where

$$\boldsymbol{\Sigma}_{\mathbf{w}_i} = (\mathbf{W}_{-i}^\top \mathbf{W}_{-i} + \mathbf{I}_H)^{-1}, \quad \boldsymbol{\mu}_{\mathbf{w}_i} = \boldsymbol{\Sigma}_{\mathbf{w}_i} (\mathbf{W}_{-i}^\top \mathbf{z}_i + \mathbf{I}_H \mathbf{a}_0),$$

and with $\text{TN}(\mu, \sigma^2, [a, b])$ denoting a truncated normal distribution with parameters (μ, σ^2) , restricted over the interval $[a, b]$. Posterior inference via MCMC relies on iterative sampling from Equation (3) or (4), constructing a Markov chain which has the joint posterior distribution $p(\mathbf{W}, \mathbf{z} \mid \mathbf{Y})$ as a limiting distribution (Gelfand and Smith, 1990). Some factors can be omitted in the expressions above; for example, $p(\mathbf{w}_i \mid \mathbf{W}_{-i}, \mathbf{z}_i, \mathbf{y}_i) = p(\mathbf{w}_i \mid \mathbf{W}_{-i}, \mathbf{z}_i)$ in Equation (4); however, this redundant notation helps to unify both algorithms under a general specification, as outlined in the following section.

2.2 Conditional conjugancy and Variational Inference

The conditional distributions for the augmented variables z_{ij} in Equation (3) and (4) can be expressed as

$$p(z_{ij} \mid \mathbf{w}_i, \mathbf{w}_j, y_{ij}) \propto \exp \{ \eta_{ij}(\mathbf{w}_i, \mathbf{w}_j) z_{ij} - \kappa[\eta_{ij}(\mathbf{w}_i, \mathbf{w}_j)] \} p(z_{ij} \mid y_{ij}), \quad i = 2, \dots, n, j = 1, \dots, i-1, \quad (5)$$

with κ denoting the log-partition function. Equation (5) allows to express the LFM with logit and probit link with the same exponential family structure. When g is the logit link, $\eta_{ij}(\mathbf{w}_i, \mathbf{w}_j) = -0.5(\mathbf{w}_i^\top \mathbf{w}_j)^2$ and $p(z_{ij} \mid y_{ij})$ corresponds to the density of a $\text{PG}(0, 1)$; when g is the probit link, $\eta_{ij}(\mathbf{w}_i, \mathbf{w}_j) = \mathbf{w}_i^\top \mathbf{w}_j$ and $p(z_{ij} \mid y_{ij})$ corresponds to the density of a $\text{TN}(0, 1, [-\infty, 0])$ if $y_{ij} = 0$ and $\text{TN}(0, 1, [0, \infty])$ if $y_{ij} = 1$.

Conditionally on the observed data, the augmented variables and the factors $\{\mathbf{w}_j\}_{j \neq i}$, the full-conditional distribution of each \mathbf{w}_i corresponds to a multivariate Gaussian density,

$$p(\mathbf{w}_i \mid \mathbf{W}_{-i}, \mathbf{z}_i, \mathbf{y}_i) \propto \exp \{ \boldsymbol{\eta}_{i1}(\mathbf{W}_{-i}, \mathbf{y}_i, \mathbf{z}_i)^\top \mathbf{w}_i + \text{vec}[\boldsymbol{\eta}_{i2}(\mathbf{W}_{-i}, \mathbf{z}_i)]^\top \cdot \text{vec}[\mathbf{w}_i \mathbf{w}_i^\top] - \kappa[\boldsymbol{\eta}_{i1}(\mathbf{W}_{-i}, \mathbf{y}_i, \mathbf{z}_i), \boldsymbol{\eta}_{i2}(\mathbf{W}_{-i}, \mathbf{z}_i)] \}, \quad i = 1, \dots, n, \quad (6)$$

where

$$\boldsymbol{\eta}_{i1}(\mathbf{W}_{-i}, \mathbf{y}_i, \mathbf{z}_i) = \mathbf{W}_{-i}^\top (\mathbf{y}_i - 0.5 \cdot \mathbf{1}_{n-1}) + \mathbf{I}_H \mathbf{a}_0, \quad \boldsymbol{\eta}_{i2}(\mathbf{W}_{-i}, \mathbf{z}_i) = -\frac{1}{2} (\mathbf{W}_{-i}^\top \text{diag}(\mathbf{z}_i) \mathbf{W}_{-i} + \mathbf{I}_H),$$

with the logit link function, and

$$\boldsymbol{\eta}_{i1}(\mathbf{W}_{-i}, \mathbf{y}_i, \mathbf{z}_i) = \mathbf{W}_{-i}^\top \mathbf{z}_i + \mathbf{I}_H \mathbf{a}_0, \quad \boldsymbol{\eta}_{i2}(\mathbf{W}_{-i}, \mathbf{z}_i) = -\frac{1}{2} (\mathbf{W}_{-i}^\top \mathbf{W}_{-i} + \mathbf{I}_H),$$

with the probit link function.

This conditional representation of the LFM facilitates the development of algorithms that exploit maximization strategies for binary regression; for example, MAP optimization via EM algorithm (McCulloch, 1994; Scott and Sun, 2013) or approximate inference via VB (Consonni and Marin, 2007; Durante and Rigon, 2019). As discussed in section 1, the focus of the mean-field VB is on finding an approximation of the posterior distribution $p(\mathbf{W}, \mathbf{z} \mid \mathbf{Y})$ within a restricted class of densities \mathcal{Q} , specified as

$$\mathcal{Q} = \left\{ q(\mathbf{W}, \mathbf{z}) : q(\mathbf{W}, \mathbf{z}) = \prod_{i=1}^n q(\mathbf{w}_i; \boldsymbol{\lambda}_i) \prod_{i=2}^n \prod_{j=1}^{i-1} q(z_{ij}; \psi_{ij}) \right\}. \quad (7)$$

Note that each factor \mathbf{w}_i is a function of its own variational parameters $\boldsymbol{\lambda}_i$; similarly, the augmented variables z_{ij} are function of the parameter ψ_{ij} . The optimal VB solution $q^*(\mathbf{W}, \mathbf{z})$ corresponds to the distribution within \mathcal{Q} that minimizes the Kullback-Leibler (KL) divergence, defined as

$$\text{KL}[q(\mathbf{W}, \mathbf{z}) || p(\mathbf{W}, \mathbf{z} | \mathbf{Y})] = \mathbb{E}_{q(\mathbf{W}, \mathbf{z})} [\log q(\mathbf{W}, \mathbf{z})] - \mathbb{E}_{q(\mathbf{W}, \mathbf{z})} [\log p(\mathbf{W}, \mathbf{z} | \mathbf{Y})], \quad q(\mathbf{W}, \mathbf{z}) \in \mathcal{Q}. \quad (8)$$

In practice, VB procedures maximize the related objective function

$$\text{ELBO}[q(\mathbf{W}, \mathbf{z})] = \mathbb{E}_{q(\mathbf{W}, \mathbf{z})} [\log p(\mathbf{W}, \mathbf{z}, \mathbf{Y})] - \mathbb{E}_{q(\mathbf{W}, \mathbf{z})} [\log q(\mathbf{W}, \mathbf{z})], \quad q(\mathbf{W}, \mathbf{z}) \in \mathcal{Q}, \quad (9)$$

which corresponds to the negative KL up to an additive constant not depending on the parameters; see, for example, Blei et al. (2017) and Bishop (2006). The mean field assumption in Equation (7) and the conditionally conjugate representation facilitate a Coordinate Ascent Variational Inference (CAVI) routine to maximize Equation (9), where each distribution is iteratively optimized with respect to the others in an iterative fashion (e.g. Bishop, 2006). The variational distributions composing the optimal solution are in the same family of the full-conditional distributions outlined in Equations (3) and (4), and their parameters can be analytically expressed in terms of variational expectations (e.g., Blei et al., 2017). Under our specification,

$$\boldsymbol{\lambda}_{i1} = \mathbb{E}_{q(\mathbf{w}_{-i}, \mathbf{z}_i)} [\boldsymbol{\eta}_{i1}(\mathbf{W}_{-i}, \mathbf{y}_i, \mathbf{z}_i)], \quad \boldsymbol{\lambda}_{i2} = \mathbb{E}_{q(\mathbf{w}_{-i}, \mathbf{z}_i)} [\boldsymbol{\eta}_{i2}(\mathbf{W}_{-i}, \mathbf{z}_i)], \quad i = 1, \dots, n \quad (10)$$

and

$$\psi_{ij} = \mathbb{E}_{q(\mathbf{w}_i, \mathbf{w}_j)} [\eta_{ij}(\mathbf{w}_i, \mathbf{w}_j)], \quad i = 2, \dots, n, j = 1, \dots, i-1. \quad (11)$$

Algorithm 3 and 4 in Appendix A.1 illustrate the CAVI algorithms for the LFM with logit and probit link function, respectively. At each iteration t , variational expectations outlined in Equations (10) and (11) are taken with respect to the currently optimized distribution $q^{(t-1)}$, iterating until convergence. Note also that at each iteration the CAVI provides a monotone sequence of the ELBO, and convergence to a local maximum is guaranteed (Blei et al., 2017; Bishop, 2006).

3 STRATIFIED STOCHASTIC VARIATIONAL INFERENCE

The CAVI algorithms introduced in section 2.2 provide efficient routines to perform approximate Bayesian inference under the LFM. However, when the number of nodes n is extremely large, computational issues might drastically limit the analysis. For example, in Step [1] of Algorithms 3 and 4, the updates of each natural parameter λ_i involve summing over $(n - 1)$ terms, with $i = 1, \dots, n$. Also, conditional conjugacy simplifies the derivation of analytical results, but it requires to update $n(n - 1)/2$ augmented observations even when the dimension H of the latent space is small, therefore exacerbating computational and storage issues. Although variational routines generally require significantly less iterations than MCMC to reach convergence, the overall complexity of the CAVI algorithms is still $\mathcal{O}(n^2)$; therefore, CAVI provides a viable solution only in settings where n is moderately large (Salter-Townshend and Murphy, 2013). In this section we introduce a novel approach that allows to approximate the posterior distribution of the LFM for large network-data.

A scalable generalization of classical CAVI is provided by Stochastic Variational Inference (SVI, Hoffman et al., 2013), where stochastic optimization (Robbins and Monro, 1951) is used to reduce the computation cost of VB routines. We follow a similar perspective and develop a stochastic VB algorithm specifically tailored for sparse network data. Following Hoffman et al. (2013), it is useful to rewrite the CAVI routines outlined in Algorithms 3 and 4 as the solutions of a system of estimating equations, obtained computing the derivatives of the ELBO with respect to the parameters of the variational distributions.

For each fixed factor $q(\mathbf{w}_i; \lambda_i)$, computing the gradient of the ELBO outlined in Equation (9) with respect to λ_i and equating to 0 leads to the following estimating equations.

$$\mathbb{E}_{q(\mathbf{w}_{-i}, \mathbf{z}_i)} [\eta_{i1}(\mathbf{w}_{-i}, \mathbf{y}_i, \mathbf{z}_i)] - \lambda_{i1} = 0, \quad \mathbb{E}_{q(\mathbf{w}_{-i}, \mathbf{z}_i)} [\eta_{i2}(\mathbf{w}_{-i}, \mathbf{z}_i)] - \lambda_{i2} = 0. \quad (12)$$

See Hoffman et al. (2013, section 2.3) for a formal proof. Step [1] of Algorithms 3 and 4 are obtained replacing the natural parameters with the quantities outlined in Equation (6), expanding expectations with the resulting Gaussian, Pölya-Gamma or Truncated Normal moments, and solving for λ_{i1} and λ_{i2} .

Faster algorithms can be obtained replacing the gradient in Equation (12) with a computationally cheaper estimate (Robbins and Monro, 1951). In this section, we develop a computationally efficient version of this algorithm based on an informative subset of nodes. We focus on the update of a generic factor \mathbf{w}_i , and denote with $\mathcal{J}_{i0} = \{j : y_{ij} = 0\}$ the set of indices associated with nodes not connected with node i . Similarly, we define $\mathcal{J}_{i1} = \{j : y_{ij} = 1\}$, with $|\mathcal{J}_{i0}| = n_{i0}$ and $|\mathcal{J}_{i1}| = n_{i1} = n - n_{i0}$; note that n_{i1}

corresponds to the degree of node i . With the logit link function, Equation (12) can be easily decomposed into the contribution of the n_{i1} nodes connected with i and the remaining, as follows.

$$\begin{aligned} & \sum_{j \in \mathcal{J}_{i1}} \mathbb{E}_{q(\mathbf{w}_j)}[\mathbf{w}_j] (y_{ij} - 0.5) + \sum_{j \in \mathcal{J}_{i0}} \mathbb{E}_{q(\mathbf{w}_j)}[\mathbf{w}_j] (y_{ij} - 0.5) + \mathbf{I}_H \mathbf{a}_0 - \boldsymbol{\lambda}_{i1}, \\ & -0.5 \left(\sum_{j \in \mathcal{J}_{i1}} \mathbb{E}_{q(\mathbf{w}_j)} [\mathbf{w}_j \mathbf{w}_j^T] \cdot \mathbb{E}_{q(z_{ij})}[z_{ij}] + \sum_{j \in \mathcal{J}_{i0}} \mathbb{E}_{q(\mathbf{w}_j)} [\mathbf{w}_j \mathbf{w}_j^T] \cdot \mathbb{E}_{q(z_{ij})}[z_{ij}] + \mathbf{I}_H \right) - \boldsymbol{\lambda}_{i2}. \end{aligned} \quad (13)$$

Similarly, with the probit link

$$\begin{aligned} & \sum_{j \in \mathcal{J}_{i1}} \mathbb{E}_{q(\mathbf{w}_j)}[\mathbf{w}_j] \cdot \mathbb{E}_{q(z_{ij})}[z_{ij}] + \sum_{j \in \mathcal{J}_{i0}} \mathbb{E}_{q(\mathbf{w}_j)}[\mathbf{w}_j] \cdot \mathbb{E}_{q(z_{ij})}[z_{ij}] + \mathbf{I}_H \mathbf{a}_0 - \boldsymbol{\lambda}_{i1}, \\ & -0.5 \left(\sum_{j \in \mathcal{J}_{i1}} \mathbb{E}_{q(\mathbf{w}_j)} [\mathbf{w}_j \mathbf{w}_j^T] + \sum_{j \in \mathcal{J}_{i0}} \mathbb{E}_{q(\mathbf{w}_j)} [\mathbf{w}_j \mathbf{w}_j^T] + \mathbf{I}_H \right) - \boldsymbol{\lambda}_{i2}. \end{aligned} \quad (14)$$

Our strategy relies on noisy estimates of Equations (13) and (14), constructed using an informative subset of nodes $\mathcal{J}_i^* = \mathcal{J}_{i1} \cup \mathcal{J}_{i0}^*$, where $\mathcal{J}_{i0}^* \subset \mathcal{J}_{i0}$ denotes a sample from \mathcal{J}_{i0} , with $|\mathcal{J}_0| = n_{i0}^* \ll n_{i0}$. Therefore, the update for each factor \mathbf{w}_i relies on the random subset \mathcal{J}_i^* , which consists of all the nodes connected with node i and a smaller subset of not connected nodes. This approach implicitly assumes that nodes $j \in \mathcal{J}_{i0}$ not connected with i provide little information about its position in the latent space, therefore we can estimate the contribution of all these disconnected nodes relying only on few units. A similar sub-sampling strategy was introduced in Raftery et al. (2012), where the authors improve MCMC computation approximating the log-likelihood with a sub-sample of informative nodes. Differently from Raftery et al. (2012), we use sampling in conjunction with stochastic optimization to efficiently obtain a VB solution, which in turn correspond to solve Equation (12) with respect to the variational parameters $(\boldsymbol{\lambda}_{i1}, \boldsymbol{\lambda}_{i2})$, for $i = 1, \dots, n$. Also, the approach developed Raftery et al. (2012) relies on specific properties of the logistic link, while our approach is more general and valid for different link functions.

A simple strategy leading to a computationally cheap estimate of Equations (13) and (14) is to construct the set \mathcal{J}_{i0}^* relying on random sampling, where each unit $j \in \mathcal{J}_{i0}$ is included in the sample with probability n_{i0}^{-1} . This choice leads to the following unbiased estimator of Equation (13), denoted as $[B(\boldsymbol{\lambda}_{i1}), B(\boldsymbol{\lambda}_{i2})]$

and corresponding to the discrete random variable taking values

$$\begin{aligned}
B_{\mathcal{J}_i^*}(\boldsymbol{\lambda}_{i1}) &= \sum_{j \in \mathcal{J}_{i1}} \mathbb{E}_{q(\mathbf{w}_j)}[\mathbf{w}_j] (y_{ij} - 0.5) + \frac{n_{i0}}{n_{i0}^*} \sum_{j \in \mathcal{J}_{i0}^*} \mathbb{E}_{q(\mathbf{w}_j)}[\mathbf{w}_j] (y_{ij} - 0.5) + \mathbf{I}_H \mathbf{a}_0 - \boldsymbol{\lambda}_{i1}, \\
B_{\mathcal{J}_i^*}(\boldsymbol{\lambda}_{i2}) &= -0.5 \left(\sum_{j \in \mathcal{J}_{i1}} \mathbb{E}_{q(\mathbf{w}_j)} [\mathbf{w}_j \mathbf{w}_j^\top] \cdot \mathbb{E}_{q(z_{ij})}[z_{ij}] + \frac{n_{i0}}{n_{i0}^*} \sum_{j \in \mathcal{J}_{i0}^*} \mathbb{E}_{q(\mathbf{w}_j)} [\mathbf{w}_j \mathbf{w}_j^\top] \cdot \mathbb{E}_{q(z_{ij})}[z_{ij}] + \mathbf{I}_H \right) - \boldsymbol{\lambda}_{i2},
\end{aligned} \tag{15}$$

for each possible $\mathcal{J}_{i0}^* \subset \mathcal{J}_{i0}$.

Similarly, for Equation (14)

$$\begin{aligned}
B_{\mathcal{J}_i^*}(\boldsymbol{\lambda}_{i1}) &= \sum_{j \in \mathcal{J}_{i1}} \mathbb{E}_{q(\mathbf{w}_j)}[\mathbf{w}_j] \cdot \mathbb{E}_{q(z_{ij})}[z_{ij}] + \frac{n_{i0}}{n_{i0}^*} \sum_{j \in \mathcal{J}_{i0}^*} \mathbb{E}_{q(\mathbf{w}_j)}[\mathbf{w}_j] \cdot \mathbb{E}_{q(z_{ij})}[z_{ij}] + \mathbf{I}_H \mathbf{a}_0 - \boldsymbol{\lambda}_{i1}, \\
B_{\mathcal{J}_i^*}(\boldsymbol{\lambda}_{i2}) &= -0.5 \left(\sum_{j \in \mathcal{J}_{i1}} \mathbb{E}_{q(\mathbf{w}_j)} [\mathbf{w}_j \mathbf{w}_j^\top] + \frac{n_{i0}}{n_{i0}^*} \sum_{j \in \mathcal{J}_{i0}^*} \mathbb{E}_{q(\mathbf{w}_j)} [\mathbf{w}_j \mathbf{w}_j^\top] + \mathbf{I}_H \right) - \boldsymbol{\lambda}_{i2}.
\end{aligned} \tag{16}$$

From a storage perspective, this representation allows to explicitly rely on the edge-list format of the network, where only the distinct pairs (i, j) associated with an edge are stored in memory. In its original formulation, SVI relies on sampling one single observation per iteration, and updating the gradient with the resulting estimate. Instead, for SVILF we recommend letting $n_{i0}^* = \min(n_{i0}, \lfloor \gamma n_{i1} \rfloor)$, with $\gamma > 1$ and where $\lfloor \gamma n_{i1} \rfloor$ denotes the greatest integer less than or equal to γn_{i1} . In sparse network settings, $n_{i0}^* \gg n_{i1}^*$ and the random subset \mathcal{J}_{i0}^* will generally consist of $n_{i0}^* = \lfloor \gamma n_{i1} \rfloor$ elements. Larger values of γ leads to estimator $[B(\boldsymbol{\lambda}_{i1}), B(\boldsymbol{\lambda}_{i2})]$ with smaller variance, while small values of γ lead to more efficient computation. In our experience, letting $\gamma \in [1, 5]$ provides good performance in a large number of applications; see sections 4 and 5.

The simple form of the proposed estimator allows the direct applications of the stochastic approximation method proposed in Robbins and Monro (1951) to solve Equation (12) via iterative updates as

$$\begin{aligned}
\boldsymbol{\lambda}_{i1}^{(t)} &= (1 - \rho_t) \boldsymbol{\lambda}_{i1}^{(t-1)} + \rho_t B_{\mathcal{J}_i^*}(\boldsymbol{\lambda}_{i1}^{(t-1)}), \\
\boldsymbol{\lambda}_{i2}^{(t)} &= (1 - \rho_t) \boldsymbol{\lambda}_{i2}^{(t-1)} + \rho_t B_{\mathcal{J}_i^*}(\boldsymbol{\lambda}_{i2}^{(t-1)}),
\end{aligned} \tag{17}$$

where $[B_{\mathcal{J}_i^*}(\boldsymbol{\lambda}_{i1}^{(t-1)}), B_{\mathcal{J}_i^*}(\boldsymbol{\lambda}_{i2}^{(t-1)})]$ denotes a draw from the estimators outlined in Equation (15) and (16) evaluated at $(\boldsymbol{\lambda}_{i1}^{(t-1)}, \boldsymbol{\lambda}_{i2}^{(t-1)})$, and ρ_t denotes a sequence of step size such that $\sum_t \rho_t = +\infty$ and $\sum_t \rho_t^2 < +\infty$ (Robbins and Monro, 1951). A standard choice is to let $\rho_t = (t + \alpha)^{-\beta}$, with $\alpha > 0$ and $0.5 < \beta < 1$ (Hoffman et al., 2013; Durante and Rigon, 2019). Recalling Appendix A of Hoffman et al. (2013), in

Equation (17) parameters λ_i are simultaneously updated to guarantee converge to the solution of (12). These optima are analytically obtained for each $q(z_{ij})$, and iteratively for $q(\mathbf{w}_i)$, conditioning on the values $\{\mathbf{w}_j\}_{j \neq i}$ at the previous iteration, with $i = 1, \dots, n$.

As discussed in Raftery et al. (2012), uniform sub-sampling of disconnected nodes might lead to a poor representation of the network structure, due to the heterogeneity in this sub-population. Raftery et al. (2012) propose a stratified sampling based on shortest path distances, but this approach requires an expensive pilot MCMC run and the computation of a dissimilarity matrix. In our approach, uniform sub-sampling often leads to good performance; see sections 4 and 5. As an alternative, we also propose an adaptive sampling mechanism, which relies on the currently estimated network structure to draw an informative sample of nodes. This adaptive strategy samples, at iteration t , each node $j \in \mathcal{J}_{i0}^\star$ with a probability proportional to

$$g^{-1} \left(\left[\boldsymbol{\mu}_i^{(t-1)} \right]^\top \left[\boldsymbol{\mu}_j^{(t-1)} \right] \right), \quad \boldsymbol{\mu}_j^{(t-1)} := \mathbb{E}_{q^{(t-1)}(\mathbf{w}_j)}[\mathbf{w}_j], \quad j \in \mathcal{J}_{i0}^\star, \quad (18)$$

which corresponds to the current prediction for the probability to observe an edge between node i and node j according to Equation (1) and (7). Therefore, we expect that nodes $j \in \mathcal{J}_{i0}^\star$ more similar to node i —according to the latent structure specification—are more likely to be sampled and contribute to the update of $q(\mathbf{w}_i; \lambda_i)$ at iteration t . It shall be noted that, from a computational perspective, this strategy requires an additional loop over $j \in \mathcal{J}_{i0}^\star$ to compute all the products outlined in Equation (18). This operation might increase the computational time in high-dimensional settings, without significantly affecting the storage; see section 4 for an empirical evaluation. With the logit link, the proposed adaptive sampling can be used modifying Equation (13) as

$$\begin{aligned} B_{\mathcal{J}_i^\star}^{\text{ADA}}(\lambda_{i1}) &= \sum_{j \in \mathcal{J}_{i1}} \mathbb{E}_{q(\mathbf{w}_j)}[\mathbf{w}_j] (y_{ij} - 0.5) + \frac{m_{i0}}{m_{i0}^\star} \sum_{j \in \mathcal{J}_{i0}^\star} \mathbb{E}_{q(\mathbf{w}_j)}[\mathbf{w}_j] (y_{ij} - 0.5) + \mathbf{I}_H \mathbf{a}_0 - \lambda_{i1}, \\ B_{\mathcal{J}_i^\star}^{\text{ADA}}(\lambda_{i2}) &= -0.5 \left(\sum_{j \in \mathcal{J}_{i1}} \mathbb{E}_{q(\mathbf{w}_j)} \left[\mathbf{w}_j \mathbf{w}_j^\top \right] \cdot \mathbb{E}_{q(z_{ij})}[z_{ij}] + \frac{m_{i0}}{m_{i0}^\star} \sum_{j \in \mathcal{J}_{i0}^\star} \mathbb{E}_{q(\mathbf{w}_j)} \left[\mathbf{w}_j \mathbf{w}_j^\top \right] \cdot \mathbb{E}_{q(z_{ij})}[z_{ij}] + \mathbf{I}_H \right) - \lambda_{i2}, \end{aligned}$$

with

$$m_{i0} := \sum_{j \in \mathcal{J}_{i0}} \left[1 + \exp \left(\left[\boldsymbol{\mu}_i^{(t-1)} \right]^\top \left[\boldsymbol{\mu}_j^{(t-1)} \right] \right) \right]^{-1}, \quad m_{i0}^\star := \sum_{j \in \mathcal{J}_{i0}^\star} \left[1 + \exp \left(\left[\boldsymbol{\mu}_i^{(t-1)} \right]^\top \left[\boldsymbol{\mu}_j^{(t-1)} \right] \right) \right]^{-1}. \quad (19)$$

Similarly, for the probit link function it holds that

$$\begin{aligned}
B_{\mathcal{J}_i^*}^{\text{ADA}}(\boldsymbol{\lambda}_{i1}) &= \sum_{j \in \mathcal{J}_{i1}} \mathbb{E}_{q(\mathbf{w}_j)}[\mathbf{w}_j] \cdot \mathbb{E}_{q(z_{ij})}[z_{ij}] + \frac{m_{i0}}{m_{i0}^*} \sum_{j \in \mathcal{J}_{i0}^*} \mathbb{E}_{q(\mathbf{w}_j)}[\mathbf{w}_j] \cdot \mathbb{E}_{q(z_{ij})}[z_{ij}] + \mathbf{I}_H \mathbf{a}_0 - \boldsymbol{\lambda}_{i1}, \\
B_{\mathcal{J}_i^*}^{\text{ADA}}(\boldsymbol{\lambda}_{i2}) &= -0.5 \left(\sum_{j \in \mathcal{J}_{i1}} \mathbb{E}_{q(\mathbf{w}_j)}[\mathbf{w}_j \mathbf{w}_j^\top] + \frac{m_{i0}}{m_{i0}^*} \sum_{j \in \mathcal{J}_{i0}^*} \mathbb{E}_{q(\mathbf{w}_j)}[\mathbf{w}_j \mathbf{w}_j^\top] + \mathbf{I}_H \right) - \boldsymbol{\lambda}_{i2},
\end{aligned}$$

with

$$m_{i0} := \sum_{j \in \mathcal{J}_{i0}} \Phi \left(\left[\boldsymbol{\mu}_i^{(t-1)} \right]^\top \left[\boldsymbol{\mu}_j^{(t-1)} \right] \right), \quad m_{i0}^* := \sum_{j \in \mathcal{J}_{i0}^*} \Phi \left(\left[\boldsymbol{\mu}_i^{(t-1)} \right]^\top \left[\boldsymbol{\mu}_j^{(t-1)} \right] \right), \quad (20)$$

where $\Phi(x)$ denotes the cumulative distribution function of a standard Gaussian evaluated at x . Pseudo code illustrating SVILF is reported in Algorithms 1 and 2. See also github.com/emanuelealiverti/svilf for a C++ implementation within and R package.

4 SIMULATION STUDIES

We conduct a simulation study to evaluate the performances of the proposed SVILF algorithms in approximating the posterior distribution of model (1), in different settings. We compare our methods with the Automated Differentiation Variational Inference algorithm (ADVI, Kucukelbir et al., 2015), available in the software STAN (Stan Development Team, 2019); this algorithm relies on a fully-factorized Gaussian approximation of the posterior distribution, whose parameters are obtained via stochastic optimization, leveraging an adaptive step-size sequence; see Kucukelbir et al. (2015) for more details. In this section, we focus on the logit link for the LFM; results for the probit link are reported in the Appendix A.2. Computational performances are evaluated in terms of memory usage, elapsed time and goodness of fit. Memory is measured in MB of used RAM, while elapsed time is evaluated in seconds to run the VB routine until convergence and to draw 2500 samples from the approximate posterior distribution. For the proposed SVILF, convergence is reached when the mean squared difference between consecutive parameter values is below 10^{-6} ; for ADVI, we follow the default implementation, in which convergence is reached when the median ELBO difference is below 10^{-2} . Predictions are evaluated in terms of adequacy in recovering the probability of observing an edge, according to different metrics. Simulations are performed on server running CentOS, equipped with a 16-cores INTEL XEON E5-2690 @ 2.90GHz and 260 GB of RAM. Code to reproduce the simulations is available at <https://github.com/emanuelealiverti/svilf>.

The simulations focus on three different data generating processes. Networks in the first scenario

Algorithm 1: SSVI for LFM with logit link.

Initialize $\{\boldsymbol{\lambda}_1^{(1)}, \dots, \boldsymbol{\lambda}_n^{(1)}\}$ and set step size sequence ρ_t .

for $t = 2$ until convergence **do**

Sample a permutation σ of $\{1, \dots, n\}$ uniformly

for $i = \sigma(1), \dots, \sigma(n)$ **do**

[1] Sampling Construct the random set $\mathcal{J}_i^* = \mathcal{J}_{i1} \cup \mathcal{J}_{i0}^*$ using uniform or adaptive subsampling

[2] Local optimization Compute the locally optimized densities for $z_{ij}, j \in \mathcal{J}_i^*$ leading to Pólya-Gamma densities with natural parameters

$$\psi_{ij}(\boldsymbol{\lambda}_i^{(t-1)}, \boldsymbol{\lambda}_j^{(t-1)}) = -0.5 \left[\text{vec}(\mathbf{S}_i^{(t-1)})^\top \text{vec}(\mathbf{S}_j^{(t-1)}) \right],$$

with

$$\mathbf{S}_j^{(t-1)} = \left(-2\boldsymbol{\lambda}_{j2}^{(t-1)}\right)^{-1} + \left[\left(-2\boldsymbol{\lambda}_{j2}^{(t-1)}\right)^{-1} \boldsymbol{\lambda}_{j1}^{(t-1)}\right]^\top \left[\left(-2\boldsymbol{\lambda}_{j2}^{(t-1)}\right)^{-1} \boldsymbol{\lambda}_{j1}^{(t-1)}\right].$$

[2] Global optimization. Update the global parameters leveraging stochastic optimization.

$$\begin{aligned} \boldsymbol{\lambda}_{i1}^{(t)} &= (1 - \rho_t) \boldsymbol{\lambda}_{i1}^{(t-1)} + \rho_t \left\{ \sum_{j \in \mathcal{J}_{i1}} \left[\left(-2\boldsymbol{\lambda}_{j2}^{(t-1)}\right)^{-1} \boldsymbol{\lambda}_{j1}^{(t-1)} \right] (y_{ij} - 0.5) + \right. \\ &\quad \left. r_{i0} \sum_{j \in \mathcal{J}_{i0}^*} \left[\left(-2\boldsymbol{\lambda}_{j2}^{(t-1)}\right)^{-1} \boldsymbol{\lambda}_{j1}^{(t-1)} \right] (y_{ij} - 0.5) + \mathbf{I}_H \mathbf{a}_0 \right\} \\ \boldsymbol{\lambda}_{i2}^{(t)} &= (1 - \rho_t) \boldsymbol{\lambda}_{i2}^{(t-1)} - \rho_t 0.5 \left(\sum_{j \in \mathcal{J}_{i1}} \mathbf{S}_j^{(t-1)} \cdot \bar{z}_{ij}^{(t-1)} + r_{i0} \sum_{j \in \mathcal{J}_{i0}^*} \mathbf{S}_j^{(t-1)} \cdot \bar{z}_{ij}^{(t-1)} + \mathbf{I}_H \right), \end{aligned}$$

with

$$\bar{z}_{ij}^{(t-1)} = \left[\psi_{ij}(\boldsymbol{\lambda}_i^{(t-1)}, \boldsymbol{\lambda}_j^{(t-1)}) \right]^{-1} \tanh \left[\psi_{ij}(\boldsymbol{\lambda}_i^{(t-1)}, \boldsymbol{\lambda}_j^{(t-1)}) \right]$$

and with $r_{i0} = n_{i0}/n_{i0}^*$ in case of uniform sampling and $r_i = m_{i0}/m_{i0}^*$ for the adaptive version, as outlined in Equation (19). Therefore, the approximating density for \mathbf{w}_i is Gaussian with mean $\boldsymbol{\mu}_i^{(t)}$ and covariance $\boldsymbol{\Sigma}_i^{(t)}$, where

$$\boldsymbol{\mu}_i^{(t)} = \left(-2\boldsymbol{\lambda}_{i2}^{(t)}\right)^{-1} \boldsymbol{\lambda}_{i1}^{(t)}, \quad \boldsymbol{\Sigma}_i^{(t)} = \left(-2\boldsymbol{\lambda}_{i2}^{(t)}\right)^{-1}.$$

Output $q^*(\mathbf{W}) = \prod_{i=1}^n q^*(\mathbf{w}_i)$.

(s1) are generated according to a LFM model, with 2 latent factors randomly generated from multivariate Gaussian with diagonal covariance and standard deviation equal to 3. In the second simulation scenario (s2), data are generated from a latent Euclidean distance model (Hoff et al., 2002) having 2-dimensional latent positions, generated from standard Gaussian distributions, while in the third and last scenario

Algorithm 2: SSVI for LFM with probit link.

Initialize $\{\boldsymbol{\lambda}_1^{(1)}, \dots, \boldsymbol{\lambda}_n^{(1)}\}$ and set step size sequence ρ_t .

for $t = 2$ until convergence **do**

for $i = 1, \dots, n$ **do**

[1] Sampling Construct the random set $\mathcal{J}_i^* = \mathcal{J}_{i1} \cup \mathcal{J}_{i0}^*$ using uniform or adaptive subsampling

[2] Local optimization Compute the locally optimized densities for $z_{ij}, j \in \mathcal{J}_i^*$ leading to Truncated Normal distributions with natural parameters

$$\psi_{ij}(\boldsymbol{\lambda}_i^{(t-1)}, \boldsymbol{\lambda}_j^{(t-1)}) = \left[\left(-2\boldsymbol{\lambda}_{i2}^{(t-1)} \right)^{-1} \boldsymbol{\lambda}_{i1}^{(t-1)} \right]^\top \left[\left(-2\boldsymbol{\lambda}_{j2}^{(t-1)} \right)^{-1} \boldsymbol{\lambda}_{j1}^{(t-1)} \right]$$

[2] Global optimization. Update the global parameters leveraging a stochastic optimization

$$\begin{aligned} \boldsymbol{\lambda}_{i1}^{(t)} &= (1 - \rho_t) \boldsymbol{\lambda}_{i1}^{(t-1)} + \rho_t \left\{ \sum_{j \in \mathcal{J}_{i1}} \left[\left(-2\boldsymbol{\lambda}_{j2}^{(t-1)} \right)^{-1} \boldsymbol{\lambda}_{j1}^{(t-1)} \right] \tilde{z}_{ij} + \right. \\ &\quad \left. r_{i0} \sum_{j \in \mathcal{J}_{i0}^*} \left[\left(-2\boldsymbol{\lambda}_{j2}^{(t-1)} \right)^{-1} \boldsymbol{\lambda}_{j1}^{(t-1)} \right] \tilde{z}_{ij} + \mathbf{I}_H \mathbf{a}_0 \right\} \\ \boldsymbol{\lambda}_{i2}^{(t)} &= (1 - \rho_t) \boldsymbol{\lambda}_{i2}^{(t-1)} - \rho_t 0.5 \left(\sum_{j \in \mathcal{J}_{i1}} \mathbf{S}_j^{(t-1)} + r_{i0} \sum_{j \in \mathcal{J}_{i0}^*} \mathbf{S}_j^{(t-1)} + \mathbf{I}_H \right), \end{aligned}$$

with

$$\mathbf{S}_j^{(t-1)} = \left(-2\boldsymbol{\lambda}_{j2}^{(t-1)} \right)^{-1} + \left[\left(-2\boldsymbol{\lambda}_{j2}^{(t-1)} \right)^{-1} \boldsymbol{\lambda}_{j1}^{(t-1)} \right]^\top \left[\left(-2\boldsymbol{\lambda}_{j2}^{(t-1)} \right)^{-1} \boldsymbol{\lambda}_{j1}^{(t-1)} \right]$$

and

$$\begin{aligned} \tilde{z}_{ij}^{(t-1)} &= \psi_{ij}^{(t-1)}(\boldsymbol{\lambda}_i^{(t-1)}, \boldsymbol{\lambda}_j^{(t-1)}) + \\ &\quad (2y_{ij} - 1) \phi \left(\psi_{ij}^{(t-1)}(\boldsymbol{\lambda}_i^{(t-1)}, \boldsymbol{\lambda}_j^{(t-1)}) \right) \Phi \left[(2y_{ij} - 1) \psi_{ij}^{(t-1)}(\boldsymbol{\lambda}_i^{(t-1)}, \boldsymbol{\lambda}_j^{(t-1)}) \right]^{-1}, \end{aligned}$$

where $\phi(x)$ and $\Phi(x)$ represent the density and the cumulative distribution function of a standard Gaussian evaluated in x , respectively, and with $r_{i0} = n_{i0}/n_{i0}^*$ in case of uniform sampling and $r_i = m_{i0}/m_{i0}^*$ for the adaptive version, as outlined in Equation (20).

Therefore, the approximating density for \mathbf{w}_i is Gaussian with mean $\boldsymbol{\mu}_i^{(t)}$ and covariance $\boldsymbol{\Sigma}_i^{(t)}$, where

$$\boldsymbol{\mu}_i^{(t)} = \left(-2\boldsymbol{\lambda}_{i2}^{(t)} \right)^{-1} \boldsymbol{\lambda}_{i1}^{(t)}, \quad \boldsymbol{\Sigma}_i^{(t)} = \left(-2\boldsymbol{\lambda}_{i2}^{(t)} \right)^{-1}.$$

Output $q^*(\mathbf{W}) = \prod_{i=1}^n q^*(\mathbf{w}_i)$.

(s3), data are generated from a stochastic block-model with 2 latent groups, equal weights, within-group probability of connection equal to 0.6 and between-group probability equal to 0.2. For each scenario, we

| | n | 100 | 200 | 300 | 500 | 1000 | 2000 | 3000 | 5000 |
|----|-------------|--------|--------|--------|--------|--------|---------|---------|---------|
| s1 | SVILF | 333.81 | 394.39 | 396.05 | 401.08 | 421.60 | 502.18 | 630.28 | 1037.75 |
| | SVILF (ADA) | 393.60 | 394.57 | 396.06 | 401.09 | 423.32 | 502.18 | 630.28 | 1037.75 |
| | ADVI | 358.91 | 368.11 | 380.89 | 408.82 | 568.11 | 1181.61 | 3210.12 | 6403.59 |
| s2 | SVILF | 309.54 | 374.38 | 396.58 | 402.96 | 426.77 | 514.90 | 675.66 | 1177.50 |
| | SVILF (ADA) | 393.78 | 395.00 | 396.58 | 402.97 | 428.79 | 514.91 | 675.66 | 1177.50 |
| | ADVI | 358.96 | 368.15 | 380.94 | 408.88 | 568.16 | 1181.68 | 3210.20 | 6403.65 |
| s3 | SVILF | 333.88 | 395.41 | 398.47 | 407.28 | 446.69 | 543.87 | 749.57 | 1433.07 |
| | SVILF (ADA) | 393.94 | 395.62 | 398.46 | 407.28 | 449.84 | 543.88 | 749.57 | 1433.07 |
| | ADVI | 358.97 | 368.16 | 380.94 | 408.88 | 568.16 | 1181.68 | 3210.19 | 6403.65 |

Table 1: Simulation study. RAM usage in MB.

focus on networks with an increasing number of nodes $n \in \{100, 200, 300, 500, 1000, 2000, 5000\}$. We fix the number of factors of the LFM $H = 4$, set $\mathbf{a}_0 = \text{logit}(1/n(n-1) \sum_{i < j} y_{ij}) \cdot \mathbf{I}_H$ to account for the overall network sparsity, and set the SVILF step-size parameters $\alpha = 1, \beta = 0.75, \gamma = 2$. Posterior inference with ADVI is performed with default parameters configuration.

We initialize the parameters of the SVILF algorithms randomly, and in most settings convergence is reached in less than 50 iterations. In contrast, ADVI often encounters severe computational issues with random initialization, failing to complete the adaptation step and not reaching convergence. To solve this issue, we initialized the parameters of the ADVI algorithm from the eigenvalues of the adjacency matrix, reaching convergence in all the considered scenarios. We tested the same initialization for the SVILF algorithms, finding no significant difference in the results.

Table 1 reports the memory usage for posterior inference in each of the considered simulation scenario. When the number of nodes is in the order of few hundreds, the considered algorithms require a similar amounts of RAM. In contrast, when the number of nodes is in the order of few hundreds, the proposed SVILF algorithms requires significantly less memory in all the scenarios. For example, in the case $n = 3000$, ADVI requires around 4 times as much memory as SVILF; this factor is increasing with n , showing the efficiency of the SVILF algorithms in large-networks settings. As expected, the two sampling schemes implemented under the SVILF algorithm perform similarly in terms of memory usage. It is worth noticing that posterior inference under SVILF does not require high-performance computational resources, since it uses at most 1.4GB of RAM with $n = 5000$ nodes.

Table 2 compares the elapsed time required by the different algorithms to reach convergence and draw 2500 samples from the approximate posterior. Results suggest that SVILF with uniform sub-sampling provides the fastest routine in all the considered settings, with an elapsed time which roughly ranges

| | n | 100 | 200 | 300 | 500 | 1000 | 2000 | 3000 | 5000 |
|----|-------------|-------|-------|--------|--------|---------|---------|----------|----------|
| s1 | SVILF | 2.01 | 3.01 | 6.51 | 19.03 | 117.18 | 997.73 | 4285.21 | 7213.88 |
| | SVILF (ADA) | 3.51 | 11.02 | 14.53 | 45.58 | 229.93 | 1419.76 | 5495.70 | 24561.37 |
| | ADVI | 5.01 | 52.11 | 114.23 | 328.67 | 1163.38 | 4632.29 | 10495.66 | 29755.55 |
| s2 | SVILF | 1.50 | 2.51 | 5.51 | 13.52 | 42.57 | 352.64 | 1397.19 | 6290.47 |
| | SVILF (ADA) | 3.51 | 10.52 | 20.54 | 59.11 | 285.05 | 1759.93 | 5611.90 | 21549.63 |
| | ADVI | 14.03 | 50.10 | 106.72 | 285.08 | 1118.29 | 4306.76 | 9652.84 | 30736.23 |
| s3 | SVILF | 2.01 | 3.02 | 6.51 | 18.03 | 57.09 | 597.63 | 2006.35 | 2942.60 |
| | SVILF (ADA) | 4.01 | 11.52 | 25.54 | 68.62 | 331.13 | 2086.61 | 5846.57 | 21465.10 |
| | ADVI | 4.51 | 49.60 | 105.72 | 289.09 | 1095.52 | 4206.08 | 9762.82 | 32000.92 |

Table 2: Simulation study. Elapsed time (in seconds)

from 2 to 15 times faster than ADVI in all settings. For example, with $n = 3000$ and data generated under a latent-distance model (s2), SVILF is 13 times faster than the competitor, reaching convergence in roughly 14 minutes versus 3 hours required by ADVI. As expected, the adaptive sampling scheme affects the execution time of the SVILF algorithm, because of the additional loop of order $\mathcal{O}(n_{i0})$ to compute the sampling weights at each iteration. However, even if this adaptive strategy is more expensive than the standard SVILF, it still provides significant computational advantages over ADVI, reducing the elapsed time by roughly a factor of 2.

In order to evaluate the quality of predictions, Table 3 compares the goodness of fit of the posterior predictive probabilities in terms of area under the ROC curve (AUC); see also Table 8 for an evaluation in terms of precision and recall. Empirical findings suggest that all approaches achieve good performance and similar results. This is not surprising, considering that the underlying statistical model is the same and that both methods rely on similar approximations of the posterior distribution. The main advantage of SVILF is to provide massive savings in terms of computational time and memory usage, achieving accurate performance in reasonable time also in large-network settings. Results for the probit link function are consistent with the discussion above; see Appendix A.2.

5 APPLICATION

We analyze three high-dimensional datasets provided by Rozemberczki et al. (2019) and freely available on the repository <http://snap.stanford.edu/data/index.html>. The main aim of this section is to show how SVILF algorithms provide accurate representations of high-dimensional network data in terms of link prediction, and investigate the latent structure provided by the LFM. The inspection of latent structure can provide insights on the community structure of the network, highlighting groups of nodes which are

| | | 100 | 200 | 300 | 500 | 1000 | 2000 | 3000 | 5000 |
|----|-------------|-------|-------|-------|-------|-------|-------|-------|-------|
| s1 | SVILF | 0.837 | 0.861 | 0.863 | 0.849 | 0.854 | 0.852 | 0.850 | 0.853 |
| | SVILF (ADA) | 0.858 | 0.859 | 0.859 | 0.845 | 0.847 | 0.849 | 0.841 | 0.846 |
| | ADVI | 0.749 | 0.870 | 0.860 | 0.848 | 0.854 | 0.853 | 0.848 | 0.854 |
| s2 | SVILF | 0.725 | 0.685 | 0.656 | 0.637 | 0.629 | 0.619 | 0.616 | 0.616 |
| | SVILF (ADA) | 0.729 | 0.691 | 0.671 | 0.662 | 0.654 | 0.651 | 0.654 | 0.656 |
| | ADVI | 0.650 | 0.663 | 0.656 | 0.666 | 0.665 | 0.665 | 0.668 | 0.671 |
| s3 | SVILF | 0.784 | 0.768 | 0.758 | 0.745 | 0.736 | 0.727 | 0.724 | 0.720 |
| | SVILF (ADA) | 0.791 | 0.771 | 0.760 | 0.747 | 0.737 | 0.728 | 0.725 | 0.721 |
| | ADVI | 0.734 | 0.738 | 0.733 | 0.728 | 0.723 | 0.717 | 0.715 | 0.713 |

Table 3: Simulation studies. AUC.

similar in the latent space (e.g. Hoff, 2019).

The first dataset involves mutual interconnections among Facebook public pages related to politicians, governmental organizations, television shows and companies; the resulting network consists of $n = 22700$ nodes corresponding to verified Facebook pages, while edges represent the mutual “likes” between these pages. The second dataset includes the mutual following relationships among $n = 37700$ users of the popular software developing platform GitHub; the main focus is studying social interaction among active users and developers. The third dataset includes $n = 11631$ articles on crocodiles from the English version of Wikipedia; an edge indicates mutual links between articles. In all the examples, we estimate an LFM using SVILF algorithms with the same settings as in the simulations studies, increasing $\gamma = 3$ to handle the massive sparsity of the networks (the average density is 0.001). Estimation is performed on a laptop with an Intel i7-7700HQ CPU and 16 GB of RAM using the logit and the probit link function. The algorithms require roughly 30 minutes to reach convergence, assessed when the mean square difference between consecutive parameters values is below 10^{-6} .

| | | LOGIT | PROBIT |
|-----------|-------------|-------|--------|
| Facebook | SVILF (ADA) | 0.855 | 0.835 |
| | SVILF | 0.678 | 0.798 |
| GitHub | SVILF (ADA) | 0.791 | 0.867 |
| | SVILF | 0.874 | 0.809 |
| Wikipedia | SVILF (ADA) | 0.757 | 0.950 |
| | SVILF | 0.867 | 0.940 |

Table 4: Application. AUC for the proposed methods.

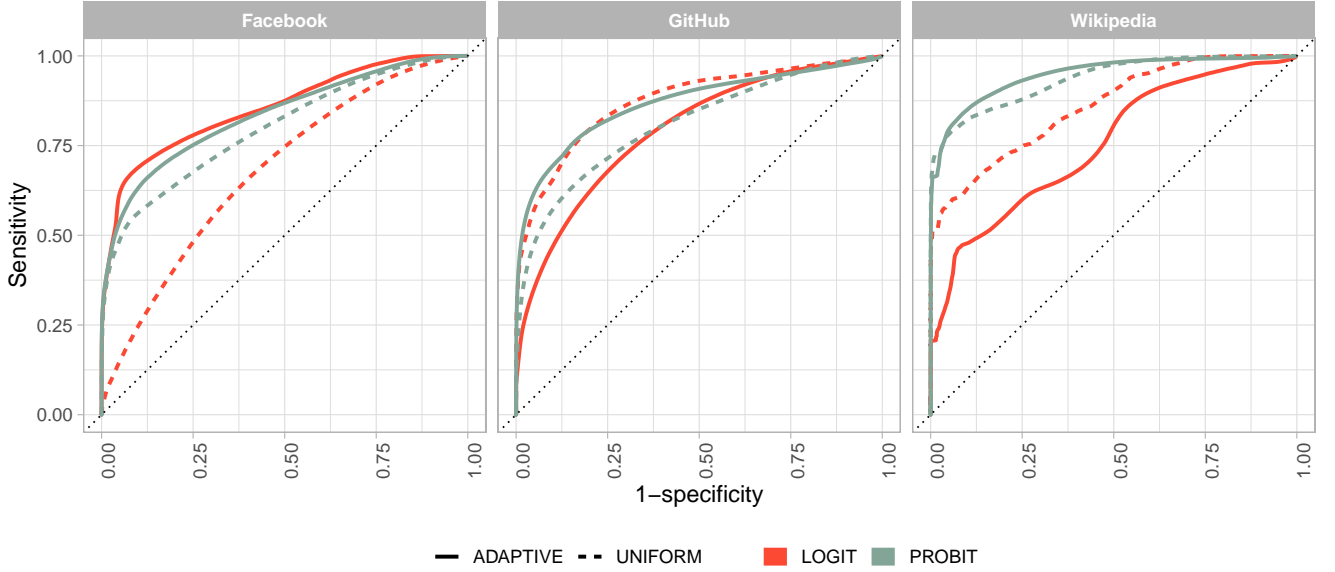


Figure 1: Application. Smoothed ROC curves for the proposed approaches over the three examples.

Figure 1 and Table 4 illustrate, respectively, the ROC curves and the AUC for the considered approaches. Results suggest a satisfactory performance for the proposed methods, with an AUC above 0.75 in most settings. Coherently with the simulations, our empirical findings do not indicate that the adaptive subsampling is systematically preferable over uniform sampling. Results from Table 4 suggest that the best-performing approach is different across applications; for example, uniform subsampling achieves lower AUC than the adaptive approach in the Facebook example, and higher in the Github dataset. Such differences might be related to the structure of network, and it will be of interest in future developments to investigate under which network structure one particular sampling approach is preferable.

Beside predictions, the LFM allows to detect latent structures via graphical inspection of the posterior means of the factors w_i , $i = 1, \dots, n$. Figure 2 illustrates the posterior means of the first two latent factors for the approaches showing higher AUC, according to Table 4. Results indicate the presence of several small clusters in the latent space, which might be interpreted as communities of nodes with similar behavior, according to the LFM. For example, in the GitHub application we highlight the presence of a large community of highly interacting users (Figure 2, center bottom), while other communities (Figure 2 top left) which are more peripheral in the latent space.

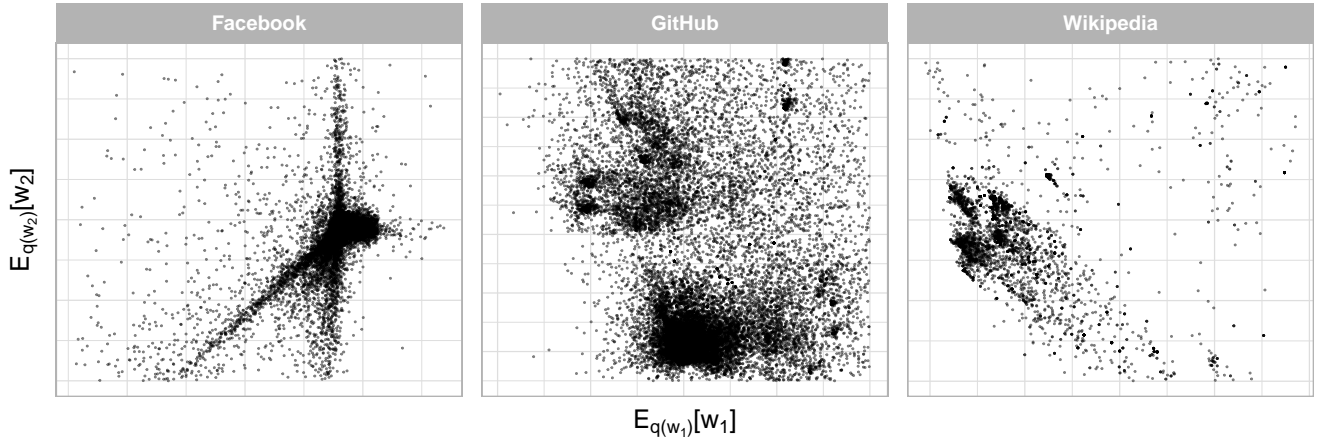


Figure 2: Application. Posterior mean for the latent factors.

6 DISCUSSION

Motivated by the abundance of large network-valued data, we have proposed a novel algorithm for posterior inference under the latent factor model for networks. Specifically, we developed a stochastic Variational Bayes routine that explicitly leverages the sparsity of high-dimensional networks to perform efficient computation. The empirical evaluations suggest that the proposed algorithms lead to significant benefits in terms of computational efficiency, without affecting accuracy in modeling the network connectivity structure.

Although the LFM is routinely used to model undirected binary networks, several applications involve more complicated structures. Some examples includes multiple networks, presence of weighted edges or the desire to include additional covariates into the analysis. The SVILF algorithms for the LFM can be directly extended to such settings considering different conditional distributions for the elements y_{ij} (e.g., Poisson or Gaussian), and allowing the probability of observing an edge to change according to some edge-specific covariate x_{ij} .

7 ACKNOWLEDGEMENTS

The work of Emanuele Aliverti was partially funded by MIUR’s PRIN 2017 project 20177BR-JXS, as well as grant grant BIRD188753/18 of the University of Padova, Italy. The authors would like to thank Peter Hoff and Daniele Durante for their comments and suggestions on the main idea of this work.

A APPENDIX

A.1 CAVI algorithms for the LFM

Algorithm 3: CAVI for LFM with logit link.

Initialize $\{\mathbf{S}_1^{(1)}, \dots, \mathbf{S}_n^{(1)}\}$ and $\{\boldsymbol{\mu}_1^{(1)}, \dots, \boldsymbol{\mu}_n^{(1)}\}$.

for $t = 2$ until convergence **do**

[1] $q^{(t)}(\mathbf{w}_i)$ is the density of a $N_H(\boldsymbol{\mu}_i^{(t)}, \boldsymbol{\Sigma}_i^{(t)})$ with $\boldsymbol{\mu}_i^{(t)} = [-2\boldsymbol{\lambda}_{i2}^{(t)}]^{-1}\boldsymbol{\lambda}_{i1}^{(t)}$, $\boldsymbol{\Sigma}_i^{(t)} = [-2\boldsymbol{\lambda}_{i2}^{(t)}]^{-1}$ and natural parameters

$$\boldsymbol{\lambda}_{i1}^{(t)} = \sum_{j \neq i} \boldsymbol{\mu}_j^{(t-1)} [y_{ij} - 0.5] + \mathbf{I}_H \mathbf{a}_0, \quad \boldsymbol{\lambda}_{i2}^{(t)} = -0.5 \left(\sum_{j \neq i} \mathbf{S}_j^{(t-1)} \cdot \bar{z}_{ij}^{(t-1)} + \mathbf{I}_H \right),$$

for $i = 1, \dots, n$. In the above expression, $\bar{z}_{ij}^{(t-1)} = 0.5[\xi_{ij}^{(t-1)}] \tanh(0.5\xi_{ij}^{(t-1)})$, where

$$\mathbf{S}_j^{(t-1)} = \left[\boldsymbol{\Sigma}_j^{(t-1)} + \left[\boldsymbol{\mu}_j^{(t-1)} \right] \left[\boldsymbol{\mu}_j^{(t-1)} \right]^\top \right], \quad \xi_{ij}^{(t-1)} = \left[\text{vec} \left(\mathbf{S}_i^{(t-1)} \right)^\top \text{vec} \left(\mathbf{S}_j^{(t-1)} \right) \right]^{\frac{1}{2}}$$

[2] $q^{(t)}(z_{ij})$ is the density of a $\text{PG}(1, \xi_{ij}^{(t)})$, for $i = 2, \dots, n$ and $j = 1, \dots, i-1$.

Output $q^*(\mathbf{W}, \mathbf{z}) = \prod_{i=1}^n q^*(\mathbf{w}_i) \prod_{i=2}^n \prod_{j=1}^{i-1} q^*(z_{ij})$.

Algorithm 4: CAVI for LFM with probit link.

Initialize $\{\mathbf{S}_1^{(1)}, \dots, \mathbf{S}_n^{(1)}\}$ and $\{\boldsymbol{\mu}_1^{(1)}, \dots, \boldsymbol{\mu}_n^{(1)}\}$.

for $t = 2$ until convergence **do**

[1] $q^{(t)}(\mathbf{w}_i)$ is a density of a $N_H(\boldsymbol{\mu}_i^{(t)}, \boldsymbol{\Sigma}_i^{(t)})$ with $\boldsymbol{\mu}_i^{(t)} = [-2\boldsymbol{\lambda}_{i2}^{(t)}]^{-1}\boldsymbol{\lambda}_{i1}^{(t)}$, $\boldsymbol{\Sigma}_i^{(t)} = [-2\boldsymbol{\lambda}_{i2}^{(t)}]^{-1}$ and

$$\boldsymbol{\lambda}_{i1}^{(t)} = \sum_{j \neq i} \boldsymbol{\mu}_j^{(t-1)} \tilde{z}_{ij}^{(t-1)} + \mathbf{I}_H \mathbf{a}_0, \quad \boldsymbol{\lambda}_{i2}^{(t)} = -0.5 \left(\sum_{j \neq i} [\boldsymbol{\Sigma}_j^{(t-1)} + (\boldsymbol{\mu}_j^{(t-1)}) (\boldsymbol{\mu}_j^{(t-1)})^\top] + \mathbf{I}_H \right),$$

for $i = 1, \dots, n$. In the above expression,

$$\tilde{z}_{ij}^{(t-1)} = \gamma_{ij}^{(t-1)} + (2y_{ij} - 1)\phi(\gamma_{ij}^{(t-1)})\Phi[(2y_{ij} - 1)\gamma_{ij}^{(t-1)}]^{-1}, \quad \gamma_{ij}^{(t-1)} = (\boldsymbol{\mu}_i^{(t-1)})^\top (\boldsymbol{\mu}_j^{(t-1)})$$

and $\phi(x)$ and $\Phi(x)$ represent the density and the cumulative distribution function of a standard Gaussian evaluated in x .

[2] $q^{(t)}(z_{ij})$, is the density of a $\text{TN}[\gamma_{ij}^{(t)}, 1, (-\infty, 0)]$ if $y_{ij} = 0$ and $\text{TN}[\gamma_{ij}^{(t)}, 1, (0, +\infty)]$ if $y_{ij} = 1$,

for $i = 2, \dots, n$ and $j = 1, \dots, i-1$.

Output $q^*(\mathbf{W}, \mathbf{z}) = \prod_{i=1}^n q^*(\mathbf{w}_i) \prod_{i=2}^n \prod_{j=1}^{i-1} q^*(z_{ij})$.

A.2 Additional simulation studies

This section provides additional details on the simulation studies described in section 4.

Table 5: Probit link. Simulation study. RAM usage in MB.

| | n | 100 | 200 | 300 | 500 | 1000 | 2000 | 3000 | 5000 |
|----|-------------|--------|--------|--------|--------|--------|--------|--------|---------|
| s1 | SVILF | 309.49 | 379.22 | 395.61 | 399.73 | 422.25 | 485.11 | 573.32 | 948.16 |
| | SVILF (ADA) | 333.82 | 394.28 | 395.61 | 399.74 | 422.26 | 485.10 | 573.32 | 948.16 |
| s2 | SVILF | 340.98 | 388.07 | 395.56 | 399.49 | 420.92 | 475.13 | 547.78 | 944.76 |
| | SVILF (ADA) | 370.13 | 394.29 | 395.56 | 399.49 | 420.92 | 475.13 | 547.78 | 944.77 |
| s3 | SVILF | 333.91 | 395.52 | 398.51 | 408.10 | 453.22 | 543.64 | 749.28 | 1432.68 |
| | SVILF (ADA) | 389.12 | 395.52 | 398.50 | 408.09 | 453.22 | 543.64 | 749.28 | 1432.69 |

Table 6: Probit link. Simulation study. Elapsed time (in seconds)

| | n | 100 | 200 | 300 | 500 | 1000 | 2000 | 3000 | 5000 |
|----|-------------|------|------|-------|-------|--------|---------|---------|----------|
| s1 | SVILF | 1.50 | 2.51 | 4.01 | 16.53 | 361.55 | 200.82 | 599.18 | 2597.70 |
| | SVILF (ADA) | 2.01 | 5.51 | 11.52 | 30.55 | 186.30 | 799.77 | 1928.15 | 7857.82 |
| s2 | SVILF | 1.50 | 2.51 | 3.01 | 6.01 | 26.55 | 252.91 | 937.74 | 4742.80 |
| | SVILF (ADA) | 2.00 | 3.51 | 6.51 | 16.03 | 87.64 | 387.13 | 1230.76 | 7680.33 |
| s3 | SVILF | 2.01 | 3.01 | 5.01 | 13.02 | 70.62 | 385.70 | 1301.60 | 4849.89 |
| | SVILF (ADA) | 2.51 | 6.51 | 13.02 | 34.55 | 197.83 | 1083.52 | 3401.31 | 12882.30 |

Table 7: Probit link. Simulation studies. AUC

| | n | 100 | 200 | 300 | 500 | 1000 | 2000 | 3000 | 5000 |
|----|-------------|-------|-------|-------|-------|-------|-------|-------|-------|
| s1 | SVILF | 0.823 | 0.875 | 0.897 | 0.891 | 0.882 | 0.901 | 0.900 | 0.902 |
| | SVILF (ADA) | 0.863 | 0.905 | 0.901 | 0.910 | 0.899 | 0.898 | 0.900 | 0.899 |
| s2 | SVILF | 0.729 | 0.720 | 0.741 | 0.707 | 0.717 | 0.721 | 0.720 | 0.716 |
| | SVILF (ADA) | 0.718 | 0.723 | 0.736 | 0.715 | 0.718 | 0.711 | 0.708 | 0.708 |
| s3 | SVILF | 0.773 | 0.758 | 0.758 | 0.743 | 0.732 | 0.725 | 0.722 | 0.718 |
| | SVILF (ADA) | 0.800 | 0.770 | 0.762 | 0.746 | 0.736 | 0.728 | 0.725 | 0.721 |

Table 8: Logit Link. Simulation studies. Recall (precision)

| | | 100 | 200 | 300 | 500 | 1000 | 2000 | 3000 | 5000 |
|----|-------------|---------------|---------------|---------------|---------------|---------------|---------------|---------------|---------------|
| s1 | SVILF | 0.890 (0.345) | 0.899 (0.381) | 0.894 (0.382) | 0.888 (0.377) | 0.885 (0.377) | 0.870 (0.387) | 0.883 (0.380) | 0.883 (0.376) |
| | SVILF (ADA) | 0.938 (0.331) | 0.917 (0.351) | 0.880 (0.382) | 0.882 (0.367) | 0.882 (0.370) | 0.871 (0.380) | 0.874 (0.372) | 0.875 (0.370) |
| | ADVI | 1.000 (0.207) | 0.795 (0.500) | 0.899 (0.365) | 0.893 (0.368) | 0.896 (0.369) | 0.886 (0.376) | 0.886 (0.374) | 0.899 (0.362) |
| s2 | SVILF | 0.914 (0.313) | 0.896 (0.324) | 0.871 (0.286) | 0.868 (0.297) | 0.902 (0.271) | 0.926 (0.267) | 0.878 (0.274) | 0.937 (0.270) |
| | SVILF (ADA) | 0.888 (0.325) | 0.867 (0.332) | 0.862 (0.289) | 0.865 (0.305) | 0.898 (0.273) | 0.927 (0.268) | 0.944 (0.267) | 0.959 (0.267) |
| | ADVI | 0.345 (0.460) | 0.493 (0.432) | 0.508 (0.383) | 0.527 (0.405) | 0.536 (0.376) | 0.548 (0.372) | 0.520 (0.386) | 0.559 (0.383) |
| s3 | SVILF | 0.764 (0.580) | 0.757 (0.602) | 0.750 (0.605) | 0.750 (0.598) | 0.751 (0.602) | 0.750 (0.600) | 0.750 (0.600) | 0.750 (0.600) |
| | SVILF (ADA) | 0.768 (0.583) | 0.758 (0.601) | 0.752 (0.606) | 0.750 (0.598) | 0.751 (0.602) | 0.750 (0.600) | 0.750 (0.600) | 0.750 (0.600) |
| | ADVI | 0.740 (0.567) | 0.754 (0.600) | 0.748 (0.604) | 0.750 (0.598) | 0.751 (0.602) | 0.750 (0.600) | 0.750 (0.600) | 0.750 (0.600) |

Table 9: Probit link. Simulation studies. Recall (precision)

| | | 100 | 200 | 300 | 500 | 1000 | 2000 | 3000 | 5000 |
|----|-------------|---------------|---------------|---------------|---------------|---------------|---------------|---------------|---------------|
| s1 | SVILF | 0.998 (0.251) | 0.998 (0.224) | 0.998 (0.242) | 0.998 (0.220) | 0.999 (0.234) | 0.998 (0.259) | 0.947 (0.378) | 0.951 (0.375) |
| | SVILF (ADA) | 1.000 (0.229) | 1.000 (0.199) | 1.000 (0.213) | 0.999 (0.190) | 0.998 (0.211) | 0.998 (0.219) | 0.933 (0.375) | 0.937 (0.374) |
| | ADVI | 0.931 (0.250) | 0.875 (0.209) | 0.946 (0.195) | 0.881 (0.195) | 0.919 (0.205) | 0.935 (0.190) | 0.922 (0.201) | 0.898 (0.204) |
| s2 | SVILF | 0.866 (0.264) | 0.888 (0.206) | 0.919 (0.200) | 0.895 (0.195) | 0.914 (0.206) | 0.905 (0.198) | 0.892 (0.206) | 0.893 (0.202) |
| | SVILF (ADA) | 0.745 (0.597) | 0.753 (0.597) | 0.752 (0.600) | 0.749 (0.597) | 0.750 (0.599) | 0.750 (0.600) | 0.750 (0.600) | 0.750 (0.600) |
| | ADVI | 0.771 (0.610) | 0.755 (0.599) | 0.753 (0.601) | 0.749 (0.597) | 0.750 (0.599) | 0.750 (0.600) | 0.750 (0.600) | 0.750 (0.600) |

REFERENCES

- Agresti, A. (2015). *Foundations of linear and generalized linear models*. John Wiley & Sons.
- Airoldi, E. M., Blei, D. M., Fienberg, S. E., and Xing, E. P. (2008). Mixed membership stochastic blockmodels. *Journal of Machine Learning Research*, 9(Sep):1981–2014.
- Albert, J. H. and Chib, S. (1993). Bayesian analysis of binary and polychotomous response data. *Journal of the American Statistical Association*, 88(422):669–679.
- Aliverti, E. and Durante, D. (2019). Spatial modeling of brain connectivity data via latent distance models with nodes clustering. *Statistical Analysis and Data Mining: The ASA Data Science Journal*, 12(3):185–196.
- Bishop, C. M. (2006). *Pattern recognition and machine learning*. Springer.
- Blei, D. M., Kucukelbir, A., and McAuliffe, J. D. (2017). Variational inference: A review for statisticians. *Journal of the American Statistical Association*, 112(518):859–877.
- Bullmore, E. and Sporns, O. (2009). Complex brain networks: graph theoretical analysis of structural and functional systems. *Nature Reviews Neuroscience*, 10(3):186.
- Consonni, G. and Marin, J.-M. (2007). Mean-field variational approximate Bayesian inference for latent variable models. *Computational Statistics & Data Analysis*, 52(2):790–798.
- Csardi, G. and Nepusz, T. (2006). The igraph software package for complex network research. *InterJournal, Complex Systems*:1695.
- Durante, D., Dunson, D. B., and Vogelstein, J. T. (2017). Nonparametric Bayes modeling of populations of networks. *Journal of the American Statistical Association*, 112(520):1516–1530.
- Durante, D. and Rigon, T. (2019). Conditionally conjugate mean-field variational Bayes for logistic models. *Statistical Science*, 34(3):472–485.
- D’Amico, S., Murphy, T. B., Alfò, M., et al. (2019). Latent space modelling of multidimensional networks with application to the exchange of votes in eurovision song contest. *The Annals of Applied Statistics*, 13(2):900–930.

- Gelfand, A. E. and Smith, A. F. (1990). Sampling-based approaches to calculating marginal densities. *Journal of The American Statistical Association*, 85(410):398–409.
- Gollini, I. and Murphy, T. B. (2016). Joint modeling of multiple network views. *Journal of Computational and Graphical Statistics*, 25(1):246–265.
- Ho, Q., Yin, J., and Xing, E. P. (2016). Latent space inference of internet-scale networks. *The Journal of Machine Learning Research*, 17(1):2756–2796.
- Hoff, P. D. (2005). Bilinear mixed-effects models for dyadic data. *Journal of the American Statistical Association*, 100(469):286–295.
- Hoff, P. D. (2008). Modeling homophily and stochastic equivalence in symmetric relational data. In *Advances in neural information processing systems*, pages 657–664.
- Hoff, P. D. (2019). Additive and multiplicative effects network models. *Statistical Science (to appear)*.
- Hoff, P. D., Raftery, A. E., and Handcock, M. S. (2002). Latent space approaches to social network analysis. *Journal of the American Statistical Association*, 97(460):1090–1098.
- Hoffman, M. D., Blei, D. M., Wang, C., and Paisley, J. (2013). Stochastic variational inference. *The Journal of Machine Learning Research*, 14(1):1303–1347.
- Keeling, M. J. and Eames, K. T. (2005). Networks and epidemic models. *Journal of the Royal Society Interface*, 2(4):295–307.
- Kucukelbir, A., Ranganath, R., Gelman, A., and Blei, D. (2015). Automatic variational inference in stan. In *Advances in neural information processing systems*, pages 568–576.
- McCulloch, C. E. (1994). Maximum likelihood variance components estimation for binary data. *Journal of the American Statistical Association*, 89(425):330–335.
- Newman, M. (2018). *Networks*. Oxford University Press.
- Nowicki, K. and Snijders, T. A. B. (2001). Estimation and prediction for stochastic blockstructures. *Journal of the American Statistical Association*, 96(455):1077–1087.
- Polson, N. G., Scott, J. G., and Windle, J. (2013). Bayesian inference for logistic models using Pólya–Gamma latent variables. *Journal of the American Statistical Association*, 108(504):1339–1349.

- Raftery, A. E., Niu, X., Hoff, P. D., and Yeung, K. Y. (2012). Fast inference for the latent space network model using a case-control approximate likelihood. *Journal of Computational and Graphical Statistics*, 21(4):901–919.
- Robbins, H. and Monro, S. (1951). A stochastic approximation method. *The Annals of Mathematical Statistics*, pages 400–407.
- Rozemberczki, B., Allen, C., and Sarkar, R. (2019). Multi-scale attributed node embedding. *arXiv preprint arXiv:1909.13021*.
- Salter-Townshend, M. and Murphy, T. B. (2013). Variational Bayesian inference for the latent position cluster model. *Computational Statistics and Data Analysis*, 57(1):661–671.
- Scott, J. G. and Sun, L. (2013). Expectation-maximization for logistic regression. *arXiv preprint arXiv:1306.0040*.
- Sewell, D. K. and Chen, Y. (2015). Latent space models for dynamic networks. *Journal of the American Statistical Association*, 110(512):1646–1657.
- Stan Development Team (2019). RStan: the R interface to Stan. R package version 2.19.2.
- Wu, J., Vallenius, T., Ovaska, K., Westermarck, J., Mäkelä, T. P., and Hautaniemi, S. (2008). Integrated network analysis platform for protein-protein interactions. *Nature Methods*, 6(1):75.
- Young, S. J. and Scheinerman, E. R. (2007). Random dot product graph models for social networks. In *International Workshop on Algorithms and Models for the Web-Graph*, pages 138–149. Springer.